Peer-reviewed version available at *Sensors* **2019**, *19*, 1096; doi:10.3390/s19051096

Article

Low Concentration Response Hydrogen Sensors Based on Wheatstone Bridge

Hongchuan Jiang [1,*], Xiaoyu Tian [1], Xinwu Deng [1], Xiaohui Zhao [1], Luying Zhang [1], Wanli Zhang [1], Jianfeng Zhang [2] and Yifan Huang [2]

[1] State Key Laboratory of Electronic Thin Films and Integrated Devices, University of Electronic Science and Technology of China, Chengdu 610054, China; hcjiang@uestc.edu.cn (H.J.); uestctxy@163.com (X.T.); xwdeng@uestc.edu.cn (X.D.); xhzhao@uestc.edu.cn (X.Z.); luyingz@163.com (L.Z.); wlzhang@uestc.edu.cn (W.Z.)

[2] National Key Laboratory of Science and Technology on Vacuum Technology and Physics, Lanzhou Institute of Physics, Lanzhou 730000, China; zhangjianfeng510@spacechina.com (J.Z.); huangyifan@spacechina.com (Y.H.)

* Correspondence: hcjiang@uestc.edu.cn; Tel.: +86-28-6183-1181

Abstract: The PdNi film hydrogen sensors with Wheatstone bridge structure were designed and fabricated by the micro-electro-mechanical system (MEMS) technology. The integrated sensors consisted of four PdNi alloy film resistors. The internal two of them were shielded with silicon nitride film and used as reference resistors, while the others were used for hydrogen sensing. The PdNi alloy films and SiN films were deposited by magnetron sputtering. The morphology and microstructure of the PdNi films were characterized with X-ray diffraction (XRD). For efficient data acquisition, the output signal was converted from resistance to voltage. Hydrogen (H_2) sensing properties of PdNi film hydrogen sensors with Wheatstone bridge structure were investigated under different temperatures (30°C, 50°C and 70°C) and H_2 concentrations (from 10 ppm to 0.4%). The hydrogen sensor demonstrated distinct response at different hydrogen concentrations and high repeatability in cycle testing under 0.4% H_2 concentration. Towards 10ppm hydrogen, the PdNi film hydrogen sensor had evident and collectable output voltage of 600 μV.

Keywords: hydrogen sensors; PdNi thin films; Wheatstone bridge; low concentration

1. Introduction

Hydrogen (H_2) is one of the most potential and cleanest energy source [1]. Considering low minimum ignition energy and wide flammable range (4–75%), the responsive sensor is essential to detect hydrogen concentration [1,2,3]. Fast and accurate detection of hydrogen concentration is vital to prevent hydrogen leakage when using liquid hydrogen and other aerospace operations in space [2]. Based on different working principles, the hydrogen sensor can be divided into electrical, electrochemical, optical type and work function based etc. Among those sensors, work function based sensors typically need to work at elevated temperature in order to maintain high sensitivity [2,13]. Due to its ambient working temperature and convenience for measurement, resistance based sensors are extensively applied [2,3,5].

In the past decades, palladium (Pd) and palladium alloy were widely used as the sensitive materials for metallic resistor type hydrogen sensor due to its high solubility for hydrogen [2,3,17,18]. Although pure Pd could deliver a high output, fast response and superior selectivity of hydrogen, there are still some shortcomings, such as structural deformations and the consequent hysteretic resistance behavior [2,3]. In order to solve these problems, nanostructured materials and Pd alloy have been used as hydrogen sensitive materials [5–12]. Ozturk et al. reported that when exposed to 10% hydrogen, the

Peer-reviewed version available at Sensors 2019, 19, 1096; doi:10.3390/s19051096

6nm Pd films deposited on flexible substrates exhibited good reversibility and good response[13]. Lee et al. reported that hydrogen absorption and desorption did not affect the macroscopic structural deformation of PdNi. The sensitivity decreased linearly with increasing Ni content in PdNi film[11]. Hoffheins et al. reported a sensor consisting of four pure resistors with Wheatstone bridge structure, two of them were shielded with the borosilicate-based glass as hydrogen permeation barrier and served as reference resistors compensating for changes in the resistance of the palladium due to temperature variations. The thick film sensor could detect hydrogen concentration at temperatures from 0 to 200℃. However, the low concentration limit for hydrogen sensing was no less than 0.5% [14]. Meanwhile, the fabrication process of the sensor was not applicable for mass production.

In this study, the PdNi film hydrogen sensor with Wheatstone Bridge structure was designed and fabricated with micro-electro-mechanical system (MEMS) technology. The integrated sensors consisted of four PdNi alloy film resistors: two of them were shielded with silicon nitride film and used as reference resistance, while the others were used for hydrogen sensing. The output resistance signal was converted to millivolt output voltage signal for easy data acquisition. In addition, the property of the sensor was ameliorated by annealing treatment. And the performances of the Wheatstone bridge thin film hydrogen sensor were characterized and discussed.

2. Materials and Methods

2.1. Design and Fabrication of the Sensor

The schematic of the hydrogen sensor is shown in Fig 1. The sample was designed within the size of 3cm× 3.25cm × 0.43 mm. Single-sided polished silicon wafers were selected as the substrates. PdNi alloy film was used as the hydrogen sensing resistor. The bond pads of the PdNi were covered with the Au film for precise resistance measurement. And line width of the PdNi line film resistance was 100 μm. The resistance of all of the resistors was designed as 8.4 kΩ.

As shown in the Fig 2, a Wheatstone bridge type hydrogen sensor was made up of four PdNi film resistors. An external voltage source U_{in} was applied to Wheatstone bridge type hydrogen sensor. The output voltage (U_{out}) can be expressed by: :

$$U_{out} = \left(\frac{R_1 + \Delta R_1}{R_1 + R_2 + \Delta R_1} - \frac{R_3}{R_3 + R_4 + \Delta R_4} \right) U_{in} - U_0 \quad (1)$$

When the resistance of four resistors is the same ($R=R_1=R_2=R_3=R_4$), it can be simplified as:

$$U_{out} = \frac{\Delta R}{2R + \Delta R} U_{in} - U_0 = \frac{\Delta R}{2R + \Delta R} U_{in} \quad (2)$$

Where U_{in} and U_0 were the voltage of external voltage source and initial bias of the Wheatstone bridge, respectively. So the output voltage U_{out} is directly related with ΔR. The output resistance signal was converted to millivolt output voltage signal for easy data acquisition.

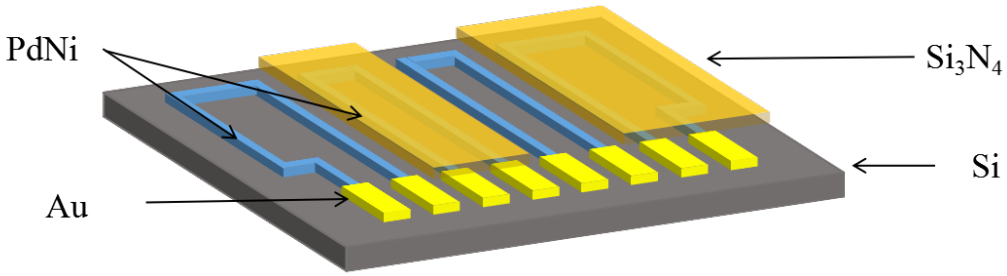

Fig 1. Schematic of the hydrogen sensors.

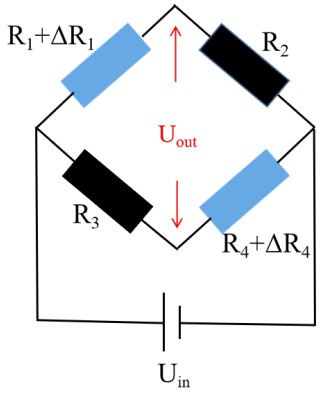

Fig 2. Structure diagram of Wheatstone bridge type hydrogen sensor

The fabrication process of the hydrogen sensor is as follows: Prior to the film deposition, the substrate was ultrasonic-cleaned successively with acetone, alcohol, and deionized water for 10 min. After that, the substrate was blow dried with nitrogen. Next, PRI-4000A photoresist was spin-coated onto the substrate and patterned with lithographic technology. Afterwards, the PdNi film with the thickness of 100 nm was deposited by DC magnetron sputtering and patterned with lift-off technique. Then the silicon nitride layer with the thickness of 160 nm was deposited by RF magnetron sputtering and patterned on the two reference resistors. At last, Au film with the thickness of 220 nm was deposited by DC magnetron sputtering and patterned on the bond pads of PdNi resistors. Sputtering parameters of all the deposition process are included in Table 1. The crystal structure of the PdNi films was examined with X-ray diffraction (XRD, Rigaku D/MAX-rA diffractometer) with the scan range from 35° to 50°.

Table 1. Sputtering parameters of different films.

Material	Base Pressure (Pa)	Sputtering Pressure (Pa)	Sputtering Power (W)	Temperature (℃)
PdNi	8×10^{-4}	0.3	60	RT
Si_3N_4	8×10^{-4}	0.5	200	RT
Au	8×10^{-4}	0.3	60	RT

After the fabrication, the sample was vacuum annealed in nitrogen for 2 hours at 300 °C. The sample was sliced into single sensor with the size of 3cm × 3.25 cm and gold wire was ball welded on the bond pad for data collection. The four resistors were connected accordingly with the external circuit to form the Wheatstone bridge. The photo of the fabricated hydrogen sensor is shown in Fig 3.

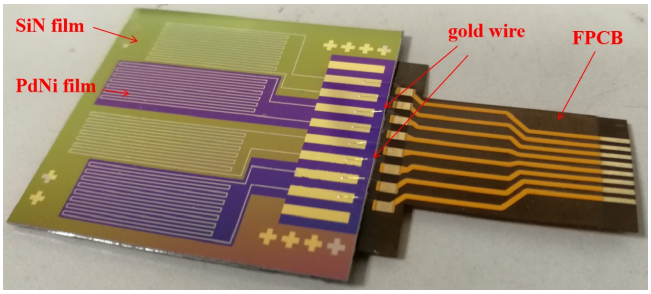

Fig 3. Photo of the fabricated hydrogen sensor.

2. Hydrogen Sensing Tests

The hydrogen measuring system consisted of mass flow controllers (MFC), gas mix chamber, gas test chamber, temperature-controlled chamber, Keithley 2182 Nanovoltmeter and the power source (Gwinstek GPC-60300), as shown in Fig 4. Before the measurement, the gas chamber was continuously purged with pure nitrogen for 2 hours with the flow rate of 100 sccm (standard cubic centimeters per minute). Next, nitrogen and hydrogen gas with different ratios was transmitted to the mix chamber. After mixing, the gas mixture was delivered to the gas chamber. The flow rate the gas mixture was controlled to be 100 sccm. The output voltage of the Wheatstone Bridge was acquired with a LabVIEW program (National Instruments) under constant voltage mode with the source voltage of 10V.

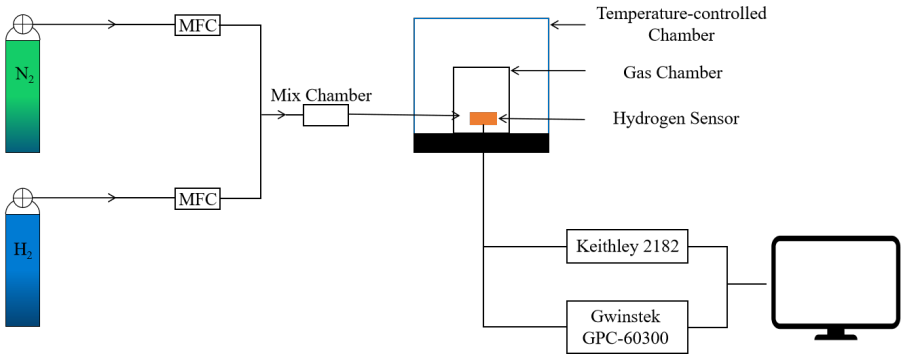

Fig 4. Schematic of the hydrogen measuring system.

3. Results and discussions

XRD pattern of the PdNi thin film was shown in Fig 5, two diffraction peaks localized at 40.64° and 47.69° reflect face-centered cubic (fcc) crystal structures of Pd and can be indexed as (111) and (200) planes, respectively. The peak positions are gradually shifted to higher angle with increasing Ni concentration in the PdNi films [11]. The full width half maximum (FWHM) of the peaks decreased after annealing, indicating the increment of the crystal size calculated with the Scherrer Equation [16].

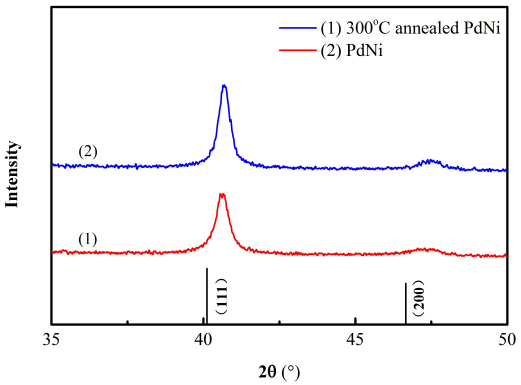

(**a**) (**b**)

Fig 5. (a) XRD patterns of (1) PdNi and (2) 300℃ annealed PdNi film; (b) SEM image of PdNi thin film.

The repeatability of the hydrogen sensor towards 0.4% hydrogen at different temperatures (30 ℃, 50 ℃ and 70 ℃) was revealed in the Fig 6. As the test temperature increases, the stability and zero drift of the sensor are partially improved despite the attenuation of the output signal. This phenomenon can be explained with the Sievert' law and Sievert constant (K) which was defined as the solubility of gas molecules in metal materials:

$$\ln \mathrm{K} = -\frac{\Delta_s H}{RT} + \frac{\Delta_s S}{R} \tag{3}$$

where $\Delta_s H$ is the molar enthalpy of solution, $\Delta_s S$ the molar entropy of solution, R the gas constant and T the environment temperature[13,15,19]. The equation (3) explained clearly that there was an inverse relationship between the temperature and sensitivity of the metal film resistance sensor [13]. The solubility of H in PdNi alloy films decreases with increased test temperature, which results in reducing maximum response of Wheatstone bridge type hydrogen sensor.

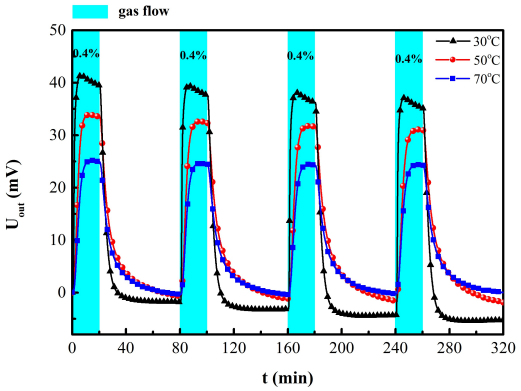

Fig 6. Repeatability of the hydrogen sensor at 30 ℃, 50 ℃ and 70 ℃ under 0.4% H_2

The response time and recovery time are defined as the consumed time to reach 90% of the final stable value [9]. When exposed to hydrogen, the output voltage of the sensor increases rapidly. After switched to pure nitrogen, the output voltage of the sensor decreases sharply, as shown in Fig 6(a), 7(a). When the hydrogen concentration increases from 200 ppm to 800 ppm, the output voltage of (2) the unannealed hydrogen sensor increased from 10.225 mV to 15.434 mV, the response time and recovery time also decreased gradually, as shown in Fig 7(a). In order to compare the two sensors under same interval test time, the unannealed sensor at 200 ppm did not reach a stable maximum response. These results indicate that with increasing hydrogen concentration, the

diffusion rate of hydrogen and the rate of hydride formation increased [2,3,4,15]. Compared with unannealed sample, the output response of the annealed sensor was somewhat reduced, however, its zero drift and repeatability were greatly improved. It has been reported that annealing treatment could alter the microstructure of Pd alloy film into influence H absorption characteristics. Hydrogen solubilities in dilute phase decrease with enhancing alloy homogeneity [20]. After annealing at 300 ℃, the PdNi peak is apparently stronger due to the grain size growth in the Fig 5(a). Due to the low annealing temperature, the microstructure of the film in the SEM image might not be significantly different. Grain size growth might be one of the factors causing change of H absorption. In addition, the internal stress in alloy film was released after annealing treatment, which might be another factor for the fast response time [17,18]. The output signal, the response

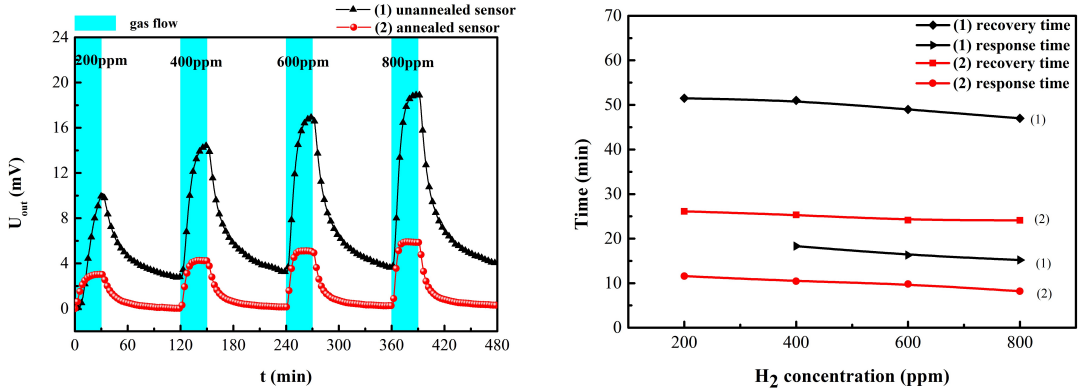

and recovery time of the annealed hydrogen sensor all decrease after annealing treatment.

Fig 7. (a) Response curve of (1) unannealed sensor and (2) annealed hydrogen sensor at 50 ℃ under different H_2 concentrations; (b) the response time and recovery time of (1) and (2).

Fig 8 (a) displays the response of the annealed hydrogen sensor at low H_2 concentration. The annealed sensor still has a detectable output voltage of 600 μV at 10ppm hydrogen. In addition, compared with single PdNi film resistance hydrogen sensor [9], the response time and recovery time of the Wheatstone bridge sensor were significantly reduced and the zero drift was greatly ameliorated. It should be noted that in sharp contrast to previous report [11,12,14], this sensor still had obvious output response under 10ppm hydrogen, which makes it applicable for wide range hydrogen concentration detection (10 ppm - 0.4 %). Furthermore, the sensor was fabricated on silicon substrates with MEMS technology, which makes it much easier for mass production and integration [21].

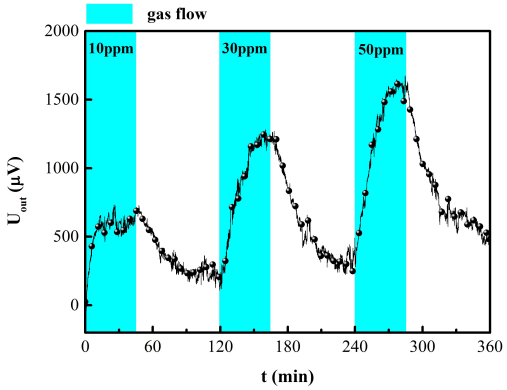

Fig 8. (a) Response curve of the annealed hydrogen sensor at 50 ℃

4. Conclusions

The highly sensitive Wheatstone bridge type hydrogen sensor based on PdNi alloy thin films was fabricated and tested. The output resistance signal was converted to millivolt output voltage signal for easy data acquisition. Compared with unannealed sample, the annealed sensor had excellent output response, faster response time and recovery time. Furthermore, the sensor demonstrated obvious output response with excellent stability and reliability over wide range of hydrogen concentration (10ppm~0.4%). This sensor was fabricated on silicon substrates with MEMS technology, which makes it much easier for mass production and integration.

Author Contributions: This work presented in this paper was a collaboration of all the authors. Hongchuan Jiang and Wanli Zhang conceived and designed the experiments; Xiaoyu Tian, Luying Zhang and Xinwu Deng performed the experiments; Hongchuan Jiang, Xiaoyu Tian and Xiaohui Zhao analyzed the data and wrote the paper; Jianfeng Zhang and Yifan Huang revised the paper.

Acknowledgments: This work was supported by the foundation of National Key Laboratory of Science and Technology on Vacuum Technology and Physics (No. ZWK1701), the National Key Research and Development Program of China (No. 2016YFB0501303).

Conflicts of Interest: The authors declare no conflict of interest.

References

1. Schlapbach, L.; Zuttel, A. Hydrogen-storage materials for mobile applications. *Nature*. **2001**, *414*, 353-8.
2. Hübert, T.; Boon-Brett, L.; Black, G.; Banach, U. Hydrogen sensors – A review. *Sens. Actuators B. Chem.* **2011**, *157*, 329-352.
3. Paglieri, S.N.; Way, J.D. Innovations in palladium membrane research. Separation & Purification Methods. **2002**, *31*, 1-169.
4. Sakamoto, Y.; Takashima, I. Hysteresis behaviour of electrical resistance of the Pd-H system measured by a gas-phase method. *Journal of Physics: Condensed Matter*. **1996**, *8*, 10511-10520.
5. Wang, B.; Zhu, Y.; Chen, Y.; Song, H.; Huang, P.; Dao, D.V. Hydrogen sensor based on palladium-yttrium alloy nanosheet. *Mater. Chem. Phys.* **2017**, *194*, 231-235.
6. Yoshimura, K.; Nakano, S.; Uchinashi, S.; Yamaura, S.; Kimura, H.; Inoue, A. A hydrogen sensor based on Mg–Pd alloy thin film. *Meas. Sci. Technol.* **2007**, *18*, 3335-3338.
7. Phan, D.-T.; Chung G.-S. Reliability of hydrogen sensing based on bimetallic Ni–Pd/graphene composites. *Int. J. Hydrogen Energ.* **2014**, *39*, 20294-20304.
8. Rashid, T.-R.; Phan, D.-T.; Chung G.-S. A flexible hydrogen sensor based on Pd nanoparticles decorated ZnO nanorods grown on polyimide tape. *Sens. Actuators B. Chem.* **2013**, *185*, 777-784.
9. Jiang, H.C.; Huang, M.; Yu, Y.B.; Tian X.Y.; Zhao X.H.; Zhang W.L.; Zhang J.F.; Huang Y.F.; Yu K. Integrated Temperature and Hydrogen Sensors with MEMS Technology. *Sensors* **2017**, *18*, 94.
10. Wadell, C.; Nugroho, F.A.A.; Lidstrom, E.; Iandolo, B.; Wagner, J. B.; Langhammer, C. Hysteresis-Free Nanoplasmonic Pd–Au Alloy Hydrogen Sensors. *Nano Lett.* **2015**, *15*, 3563-3570.
11. Lee, E.; Lee, J.M.; Lee, E.; Noh, J.; Joe, J.H.; Jung, B.; Lee, W. Hydrogen gas sensing performance of Pd–Ni alloy thin films. *Thin Solid Films*. **2010**, *519*, 880-884.
12. Chachuli, S.A.M.; Hamidon, M.N.; Mamat, M.S.; Ertugrul, M.; Abdullah, N.H. A Hydrogen Gas Sensor Based on TiO_2 Nanoparticles on Alumina Substrate. *Sensors* **2018**, *18*.
13. Ozturk, S.; Kilinc, N. Pd thin films on flexible substrate for hydrogen sensor. *J. Alloy. Compd*. **2016**, *674*, 179-184.
14. Hoffheins, B.S.; Maxey, L.C.; Jr., H.W.; Lauf R.J.; Salter C.;Walker, D. Development of low cost sensors for hydrogen safety application. Proc. of the 1999 U.S. DOE Hydrogen Program Rev. NREL/CP-570-269.
15. Jewell, L.L.; Davis, B.H. Review of Absorption and Adsorption in the Hydrogen–Palladium System. *Applied Catalysis A: General*. **2006**, *310*, 1-15.
16. Monshi, A.; Foroughi, M.R.; Monshi, M.R. Modified Scherrer Equation to Estimate More Accurately Nano-Crystallite Size Using XRD. *World Journal of Nano Science and Engineering*. **2012**, *02*, 154-160.

17. Zhao, Z.; Carpenter, M.A. Annealing enhanced hydrogen absorption in nanocrystalline Pd/Au sensing films. *J. Appl. Phys.* **2005**, *97*, 124301.
18. Hao, M.M.; Wu S.H.; Han Z.; Ye W.B., Wei, X.B.; Wang, X.R.; Zhi, C; Li, S.B. Room-temperature and fast response hydrogen sensor based on annealed nanoporous palladium film. *J. Mater. Sci.* **2016**, *51*, 2420-2426.
19. Wicke, E.; Brodowsky, H.; Zuchner, H. Hydrogen in Palladium and Palladium Alloys. *Metal Finishing* **1996**, 95, 73-155.
20. Noh, H.; Luo, W.F.; Flanagan, T.B. The Effect of Annealing Pretreatment of Pd-Rh Alloys on Their Hydrogen Solubilities and Thermodynamic Parameters for H_2 Solution. *J. Alloy. Compd.* **1993**, *196*, 7-16.
21. Nabki, F.; Allidina, K.; Ahmad, F.; Cicek, P.V.; El-Gamal, M.N. A Highly Integrated 1.8 Ghz Frequency Synthesizer Based on a Mems Resonator. *Ieee J. Solid-St. Circ.* **2009**, *44*, 2154-2168.